Quantum Mechanical Investigation of the Effect of Catalyst Fluorination in the Intermolecular Asymmetric Stetter Reaction

ARTICLE *in* JOURNAL OF THE AMERICAN CHEMICAL SOCIETY · JUNE 2011

Impact Factor: 12.11 · DOI: 10.1021/ja202444g · Source: PubMed

5 AUTHORS, INCLUDING:

Daniel Dirocco
Merck
22 PUBLICATIONS **830** CITATIONS
SEE PROFILE

Elizabeth Noey
University of California, Los Angeles
8 PUBLICATIONS **242** CITATIONS
SEE PROFILE

Tomislav Rovis
Colorado State University
180 PUBLICATIONS **7,742** CITATIONS
SEE PROFILE

Published in final edited form as:
J Am Chem Soc. 2011 July 27; 133(29): 11249–11254. doi:10.1021/ja202444g.

Quantum Mechanical Investigation of the Effect of Catalyst Fluorination in the Intermolecular Asymmetric Stetter Reaction

Joann M. Um, **Daniel A. DiRocco**, **Elizabeth L. Noey**, **Tomislav Rovi**, and **K. N. Houk**
University of California, Los Angeles, Department of Chemistry and Biochemistry, Los Angeles, CA 90095-1569

Colorado State University, Chemistry Department, Fort Collins, CO 80523

Tomislav Rovi: rovis@lamar.colostate.edu; K. N. Houk: houk@chem.ucla.edu

Abstract

The asymmetric intermolecular Stetter reaction was investigated using the B3LYP and M06-2X functionals. Fluorination of a triazolium bicyclic catalyst had been found to significantly influence reaction yields and enantiomeric ratios. Computations indicate that the improved reactivity of the fluorinated catalyst is due to better electrostatic interactions between the nitroalkene and catalyst. Computational investigations of preferred conformations of the ground state catalyst and acyl anion equivalent, and the transition structures leading to both enantiomers of the products, are reported.

Introduction

The Stetter reaction inverts the normal mode of reactivity of aldehydes by generating acyl-anion equivalents capable of reacting with Michael acceptors.[1] Following seminal work by Enders,[2] the Rovis group and others have shown that the reaction can be organocatalyzed in excellent yields and stereoselectivities.[3,4] In a recent study of the reaction of picolinaldehyde **1** and β-cyclohexyl nitroalkene **2**, DiRocco *et al.* found that fluorination of bicyclic triazolium catalysts has a significant effect on the reaction yield and enantiomeric ratios (Scheme 1).[5]

The isopropyl-substituted triazolium catalyst **4** gave promising yields and enantioselectivity.[2b] Introduction of a fluorine *cis* to the isopropyl group of **4** resulted in a catalyst (**5**) that gave improved yield and enantioselectivity results, while placement of a fluorine group *trans* to the isopropyl group of **4** gave **6**, which displayed a significant decrease in yield and no change in enantioselectivity.[5] Rovis proposed that the varying reactivities were controlled by stereoelectronic effects suggested by Raines, who has shown that fluorine has a stereoelectronic effect on the preferred conformation of proline and the stabilities of fluorinated collagen models.[6] Due to the gauche effect,[7] fluorine-substituted prolines prefer an axial-fluoride conformation. In other words, (4*S*)-isomer **flp** (Scheme 2) prefers the *endo* conformation, while (4*R*) isomer **Flp** prefers the *exo* conformation.

We reasoned that the same stereoelectronic effect should influence the preferred conformations of catalysts **4**–**6** (Figure 1). For catalyst **4**, the *endo* conformation (**4**-endo) is expected to be favored due to 1,3-diaxial strain between the isopropyl group and a hydrogen

Correspondence to: Tomislav Rovi, rovis@lamar.colostate.edu; K. N. Houk, houk@chem.ucla.edu.

Supporting Information Available. Complete ref 11 and Cartesian coordinates of all reported structures. This material is available free of charge via the Internet at http://pubs.acs.org.

in the *exo* conformation (**4**-exo). Catalyst **5** is expected to prefer the *exo* conformation (**5**-exo) because of the gauche effect of fluorine. Catalyst **6** is expected to favor the *endo* conformation (**6**-endo) both because of 1,3-diaxial strain in **6**-exo, and because of the favorable gauche effect in **6**-endo. Crystal structures of **4–6** were obtained by Rovis' group; all three structures match the preferred conformations described by Rovis in Figure 1.[5]

Computational Methods

We undertook computational studies to explore this hypothesis and to determine the effect of conformation on selectivity.[8] All geometries were optimized in the gas phase using B3LYP[9]/6-31G(d)[10] as implemented in the Gaussian 03 and 09[11] suite of programs. All stationary points were verified as minima or first-order saddle points by vibrational frequency analysis. Single point calcuations on the transition structures were performed using M06-2X[12]/6-31+G(d)[13] as implemented in Gaussian 09. Solvation free energies were calculated using the CPCM model [14] (UAKS radii, methanol, ε = 32.6). DFT calculations have provided insight into the Stetter reaction and related reactions.[8,15] Dudding and Houk predicted the stereochemistry of asymmetric benzoin reactions although with slightly overestimated *ee*.[15] While B3LYP has come under criticism for inaccuracies in reaction energy for reactions involving the transformation from π to σ bonds, a recent review validates these methods for prediction of transition state energies.[16] Furthermore, M06-2X has proven to be capable of reproducing selectivites and thermochemistries when dispersion energies are important. M06-2X results are given here in addition to B3LYP.[17]

Results and Discussion

Figure 2 shows the computed *exo* and *endo* conformers of the catalysts, **4–6**. The B3LYP/6-31G(d) lowest energy conformers are the same as those found in the crystal structures, although the preference for **4**-endo is only 0.2 kcal/mol (Figure 2). In addition to the gauche effect, the relative stabilities of the preferred conformers of **5** and **6** may be due to the distance between the pyrrolidine fluorine and the triazole N1 (labeled in Figure 2).[18] The pyrrolidine fluorine of **5** is farther from the triazole N1 in the *exo* (dihedral F-C3-C2-N1 = 73°; F–N1 = 3.20 Å) versus *endo* (dihedral F-C3-C2-N1 = 50°; F–N1 = 3.12 Å) conformation. Similarly, the pyrrolidine fluorine of **6** is farther from the triazole N1 in the *endo* (dihedral F-C3-C2-N1 = 77°; F–N1 = 3.21 Å) versus *exo* (dihedral F-C3-C2-N1 = 51°; F–N1 = 3.11 Å) conformation.

The conformations of the intermediates (**7–9**) formed by reaction of catalysts **4–6** and aldehyde **1** (Figure 3) were investigated next. Interestingly, no minima for the *endo* conformers could be located. Optimizations beginning from *endo* conformations consistently converge to the *exo* conformations. This is likely due to unfavorable interactions between the isopropyl group and enol moieties in the *endo* conformations. We therefore calculated the relative stabilities of related intermediates in which the isopropyl group was replaced by hydrogen (**10–12**, Figure 4). The fluorine has a small effect on conformation, as reflected in the small energy difference between *exo* and *endo* in **11–12**. Recent studies support this finding, showing that different conformations about the N-C-C-F dihedral angle in *E*-α-fluoro-imines have small energy differences.[19] The *endo* conformations of all three catalysts were located and are low in energy, supporting the hypothesis that an unfavorable interaction must exist between the isopropyl and enol moieties of **7–9**-endo.

To quantify the extent of steric strain in **7–9**-endo, isopropyl groups were placed on **10–12**, the *endo* geometries of the bicyclic triazoline were frozen, and the resulting structures were optimized (**7–9**-endo', Figure 5). Intermediates **7–9**-endo' are all approximately 5–7

kcal·mol^{-1} higher in energy than their corresponding *exo* conformers. The instability can be attributed to (1) H-H steric clash between the isopropyl group and the pyrrolidine ring, and (2) disfavored interaction between the isopropyl hydrogen and enol oxygen.[20] Thus, the *exo* conformations of **7–9** are strongly favored regardless of the catalyst used. *Endo* conformations **7–9**-endo' are too high in energy to be involved in the reaction. The experimentally observed stereoselectivities are attributed not to the conformation of the catalyst, but rather to (1) a steric effect, (2) a stereoelectronic effect, or (3) a combination of both, of the fluorine atom in the transition state.

Compounds **7–9** are cyclic hydrazones, and the trisubstituted nitrogen in such compounds is pyramidal.[8] The conformation of **7–9**-exo with the nitrogen pyramidalized so that C6F5 is in an “up” position is more stable than the “down” position by no more than 0.3 kcal/mol (Figure 3). The inversion barrier for the nitrogen bearing the C_6F_5 was calculated to be 5.1 kcal/mol for **8**-exo. The *Z*-isomers (not shown) are 2–3 kcal/mol higher in energy than the corresponding *E* isomers.

B3LYP gives a planar geometry of the nitrogen connected to the aromatic ring in the triazolium catalysts, **4–6**, and a tetrahedral geometry at this nitrogen in the acyl anion equivalents, **7–9**. It was brought into question whether the nitrogen in the acyl anion equivalents is truly tetrahedral or if it is analogous to the gold-coordinated triazole carbene, **13**, which is planar (Figure 6). In order to verify that our theoretical methods give reasonable geometries, we compared the crystal structure of the gold-coordinated triazole carbene, **13**, to the geometry of that given by B3LYP/6-31G(d) (/LANL2DZ for gold). Figure 6 shows that there is excellent agreement between these two geometries. It is clear that the nitrogen connected to the aromatic ring is planar in both structures.

Transition structures for Michael addition of enol intermediates **7–9** to β-cyclohexyl nitroalkene, **2**, were next located. The pentafluorophenyl group was modeled by a phenyl group. All lowest energy transition structures for addition to the *Si*-face of the nitroalkene (**TS1, TS3**, and **TS5**, favored, Figure 7) exhibit a stabilizing interaction between the hydrogen of the hydroxyl group and the carbon α–to the nitro group, in a transition state reminiscent of the reverse Cope elimination[21] as previously proposed by Rovis.[22] Similarly, the lowest energy transition structures for addition to the *Re*-face of the nitroalkene (disfavored, **TS2, TS4**, and **TS6**) show a stabilizing interaction between the hydroxy group and an oxygen of the nitro group. Transition structures for **7–9** are shown in Figures 8–10, respectively. Transition structures **TS1–TS6** are all in agreement with Seebach’s topological rule, which describes a preferred gauche arrangement of the double bonds of donors and acceptors in Michael addition transition states, including the addition of enamines to nitroalkenes (Figure 11).[23]

The experimental and calculated enantiomeric ratios are summarized in Table 1. The M06-2X activation barriers are approximately 15 kcal·mol^{-1} higher in energy than the B3LYP barriers. Furthermore, the barriers for catalyst **6**, which experimentally reacted in only 22% yield, are approximately 1 kcal·mol^{-1} higher in energy than the barriers for **4** and **5**. An examination of the transition structures led to our hypothesis for the experimentally observed enantioselectivities. We propose that **5** is more effective than **4** and **6** because the electronegative fluorine promotes a stronger attractive interaction between the developing cationic character of the catalyst bicycle and the developing anionic character of the nitroalkene in the transition state. The distances between an oxygen of the nitroalkene and the positively charged carbons of the catalyst are shorter in **TS3** (4.10 Å and 3.35 Å) compared to **TS1** (4.19 Å and 3.44 Å) and **TS5** (4.21 Å and 3.46 Å). The same holds true for the disfavored transition states. The O-C3 and O-C2 distances in **TS4** are 4.43 Å and 4.48 Å, compared to 4.63 Å and 4.68 Å in **TS2** and 4.60 Å and 4.67 Å in **TS6**. Catalyst **6** is

not as effective as **5** because the fluorine projects toward the same face as the nitroalkene, and a repulsive interaction makes this arrangement less favorable. Furthermore, **9**-exo is 1.0 kcal·mol^{-1} less stable than **8**-exo due to the disfavored F-N1 distances described earlier. This difference carries over to the transition states (Table 2).

All *Re*-face transition structures are higher in energy than the *Si*-face transition structures because of poorer stabilization of the nitroalkene by the catalyst in the latter. The nitro group of the disfavored transition structures is rotated away from the catalyst, causing the distances between an oxygen of the nitro group and the partially positive carbons of the catalyst to be longer in **TS2, TS4**, and **TS6** compared to **TS1, TS3**, and **TS5** (Figures 8–10).

Triazolium catalysts, **4–6**, can competitively catalyze the benzoin condensation over the Stetter reaction. In the case reported here, a 1.5:1 ratio of nitroalkene to aldehyde was sufficient to achieve good yields.[5] The benzoin condensation of enol intermediate, **8**, with aldehyde **1** was found to have a lower barrier than the Stetter reaction of **8** with β-cyclohexyl nitroalkene, **2** ($\Delta\Delta G^{\ddagger}$ = 2.9 kcal/mol (B3LYP) or 0.7 kcal/mol (M06-2X)). These calculations appear to overestimate the preference for the benzoin condensation. Figure 12 shows the transition state for the Stetter reaction, **TS3** (*Si*), and benzoin condensation, **TS7** (*Si*).

In conclusion, crystal structure and DFT analyses show that the preferred conformation of fluorinated triazolium catalysts **5–6** is controlled by stereoelectronic effects. Formation of the acyl anion equivalent results exclusively in the *exo* conformation of the pyrrolidine ring, regardless of the catalyst used. The favored transition structures are stabilized by an interaction between the developing negative charge in the nitro group of the alkene and the developing positive charge on the catalyst. The fluorinated catalyst, **5**, is more effective than **4** due to the electronegativity of **5**. Catalyst **6** is less effective than **5** because of unfavorable electrostatic interactions between the fluorine and both the nitroalkene and a triazolium nitrogen. The synthesis of bridged bicyclic catalysts containing methylene groups and oxygen atoms in lieu of fluorine is currently underway. Testing these catalysts should give further insight into the effect of electronegative groups on reactivity and stereoselectivity.

Supplementary Material

Refer to Web version on PubMed Central for supplementary material.

Acknowledgments

We are grateful to the National Institute of General Medical Sciences of the National Institutes of Health (GM 36700 to KNH and GM 72586 to TR), the NIH Chemistry-Biology Interface Training Program Grant (T32GM008496) and Novartis (ACS Division of Organic Chemistry Fellowship) for support of this work. Computations were performed on the TeraGrid resources provided by NCSA (CHE0400414) and the UCLA Academic Technology Services (ATS) Hoffman2 and IDRE clusters.

References

1. (a) Stetter H, Schreckenberg M. Angew. Chem., Int. Ed. Engl. 1973; 12:81.(b) Stetter H. Angew. Chem., Int. Ed. Engl. 1976; 15:639.(c) Stetter H, Kuhlmann H. Org. React. 1991; 40:407.
2. (a) Enders D, Breuer K, Runsink J, Teles JH. Helv. Chim. Acta. 1996; 79:1899.(b) Enders, D.; Breuer, K. Comprehensive Asymmetric Catalysis. Berlin: Springer; 1999. p. 1093(c) Enders D, Balensiefer T. Acc. Chem. Res. 2004; 37:534. [PubMed: 15311952] (d) Enders D, Han J, Henseler A. Chem. Commun. 2008:3989.(e) Enders D, Han J. Synthesis. 2008:3864.
3. For an account, see: Read de Alaniz J, Rovis T. Synlett. 2009:1189. [PubMed: 20585467] . For more recent work, see: (a) Liu Q, Perreault S, Rovis T. J. Am. Chem. Soc. 2008; 130:14066. [PubMed: 18834123] (b) Liu Q, Rovis T. Org. Lett. 2009; 11:2856. [PubMed: 19507841] (c)

Jousseaume T, Wurz NE, Glorius F. Angew. Chem. Int. Ed. 2011; 50:1410. (d) Dresen C, Richter M, Pohl M, Lüdeke S, Müller M. Angew. Chem. Int. Ed. 2010; 49:6600. (e) Moore JL, Silvestri AP, Read de Alaniz J, DiRocco DA, Rovis T. Org. Lett. 2011; 13:1742. [PubMed: 21355598] (f) Piel I, Steinmetz K, Hirano K, Fröhlich R, Grimme S, Glorius F. Angew. Chem. Int. Ed. 2011; 50:4983. (g) Hirano K, Biju AT, Piel I, Glorius F. J. Am. Chem. Soc. 2009; 131:14190. [PubMed: 19807174] .

4. For reviews on carbene catalysis, see: (a) Christmann M. Angew. Chem. Int. Ed. 2005; 44:2632. (b) Enders D, Niemeier O, Henseler A. Chem. Rev. 2007; 107:5606. [PubMed: 17956132] (c) Moore JL, Rovis T. Top. Curr. Chem. 2009; 290:77..
5. DiRocco DA, Oberg KM, Dalton DM, Rovis T. J. Am. Chem. Soc. 2009; 131:10872. [PubMed: 19722669]
6. (a) Bretscher LE, Jenkins CL, Taylor KM, DeRider ML, Raines RT. J. Am. Chem. Soc. 2001; 123:777. [PubMed: 11456609] (b) Hodges JA, Raines RT. J. Am. Chem. Soc. 2003; 125:9262. [PubMed: 12889933] (c) Hodges JA, Raines RT. J. Am. Chem. Soc. 2005; 127:15923. [PubMed: 16277536]
7. Wolfe S. Acc. Chem. Res. 1972; 5:102.
8. For a recent DFT study on the mechanism of the Stetter reaction, see: Hawkes KJ, Yates BF. Eur. J. Org. Chem. 2008; 33:5563..
9. (a) Becke AD. J. Chem. Phys. 1993; 98:5468.(b) Becke AD. J. Chem. Phys. 1993; 98:1372.(c) Lee C, Yang W, Parr RG. Phys. Rev. B. 1988; 98:785.
10. (a) Ditchfield R, Hehre WJ, Pople JA. J. Chem. Phys. 1971; 54:724.(b) Hehre WJ, Ditchfield R, Pople JA. J. Chem. Phys. 1972; 56:2257.(c) Hariharan PC, Pople JA. Theor. Chim. Acta. 1973; 28:213.
11. (a) Frisch, MJ., et al. Gaussian 03, revision C.02. Wallingford CT: Gaussian, Inc.; 2004. (b) Frisch, MJ., et al. Gaussian 09, revision A.1. Wallingford CT: Gaussian, Inc.; 2009.
12. (a) Zhao Y, Truhlar DG. Theor. Chem. Acc. 2008; 120:215.(b) Zhao Y, Truhlar DG. Acc. Chem. Res. 2008; 41:157. [PubMed: 18186612]
13. (a) Clark T, Chandrasekhar J, Spitznagel GW, Schleyer PvR. J. Comput. Chem. 1983; 4:294.(b) Frisch MJ, Pople JA, Binkley JS. J. Chem. Phys. 1984; 80:3265.(c) Latajka Z, Scheiner S. Chem. Phys. Lett. 1984; 105:435.
14. (a) Barone V, Cossi M. J. Phys. Chem. A. 1998; 102:1995.(b) Cossi M, Rega N, Scalmani G, Barone V. J. Comput. Chem. 2003; 24:669. [PubMed: 12666158]
15. Dudding T, Houk KN. PNAS. 2004; 101:5770. [PubMed: 15079058]
16. Simon L, Goodman JM. Org. Biomol. Chem. 2011; 9:689. [PubMed: 20976314]
17. Zhao Y, Truhlar DG. Acc. Chem. Rev. 2008; 41:157.
18. Sum of fluorine-nitrogen van der Waals radii = 3.02 Å
19. Sparr C, Salamanova E, Schweizer WB, Senn HM, Gilmour R. Chem. Eur. J. 2011 *In press*.
20. Sum of hydrogen-hydrogen van der Waals radii = 2.40 Å; sum of oxygen-hydrogen van der Waals radii = 2.72 Å
21. (a) Niu D, Zhao K. J. Am. Chem. Soc. 1999; 121:2456.(b) Sibi MP, Liu M. Org. Lett. 2000; 21:3393. [PubMed: 11029219] (c) Sibi MP, Prabagaran N, Ghorpade SG, Jasperse CP. J. Am. Chem. Soc. 2003; 125:11796. [PubMed: 14505383]
22. The intramolecular asymmetric Stetter has been demonstrated to proceed in high diastereoselectivity when using trisubstituted Michael acceptors. See: Read de Alaniz J, Rovis T. J. Am. Chem. Soc. 2005; 127:6284. [PubMed: 15853335] .
23. Seebach D, Golinski J. Helv. Chim. Acta. 1981; 64:1413.

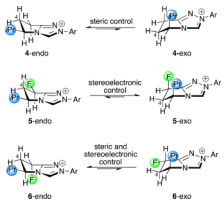

Figure 1.
Preferred conformations of triazolium catalysts **4–6**.

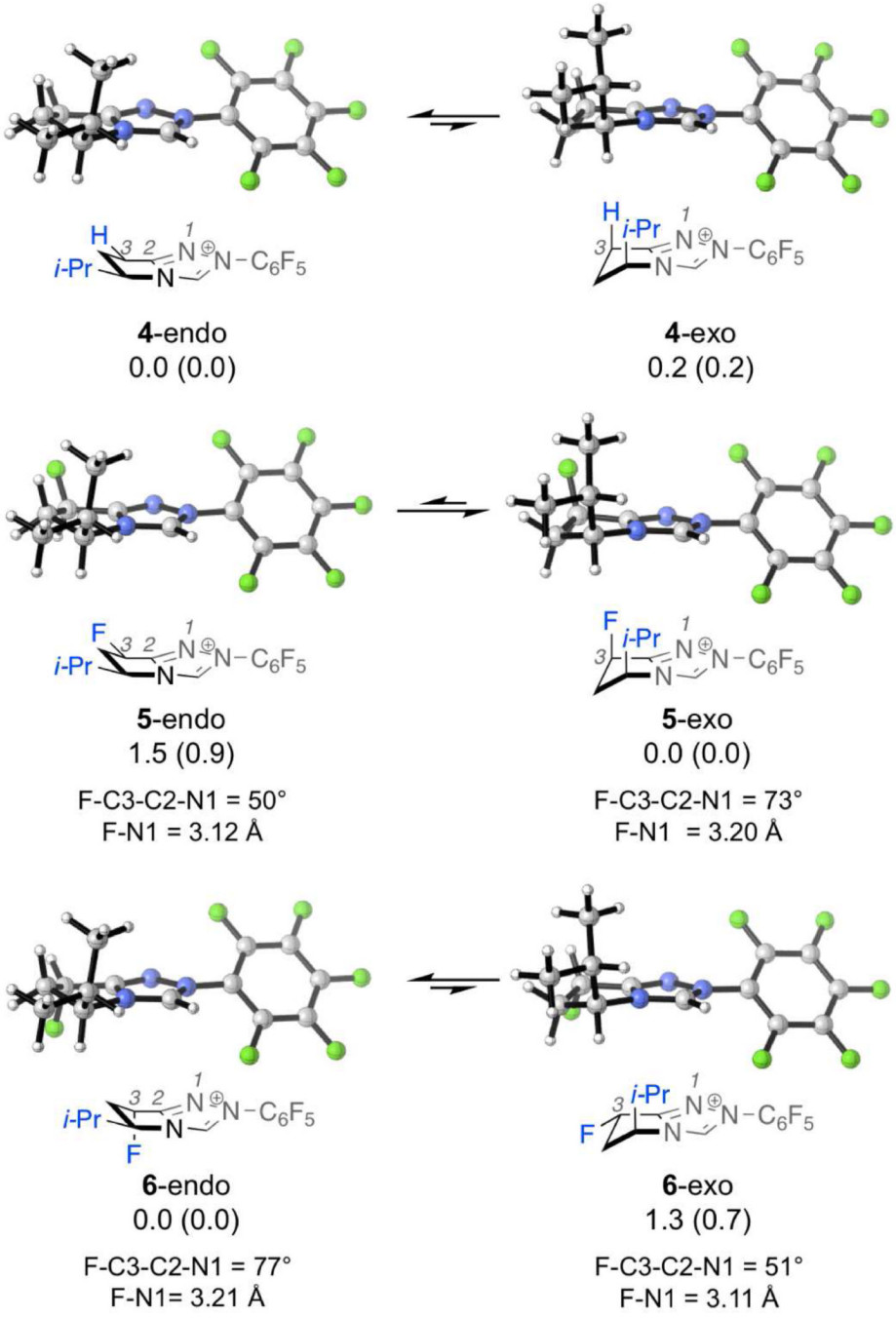

Figure 2.

B3LYP/6-31G(d) gas phase conformations and relative enthalpies of triazolium catalysts **4–6**. B3LYP/6-31+G(d) relative enthalpies with solvation corrections (CPCM methanol) are in parentheses.

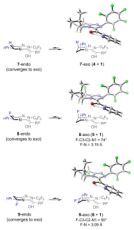

Figure 3.
B3LYP/6-31G(d) acyl anion equivalents **7–9**.

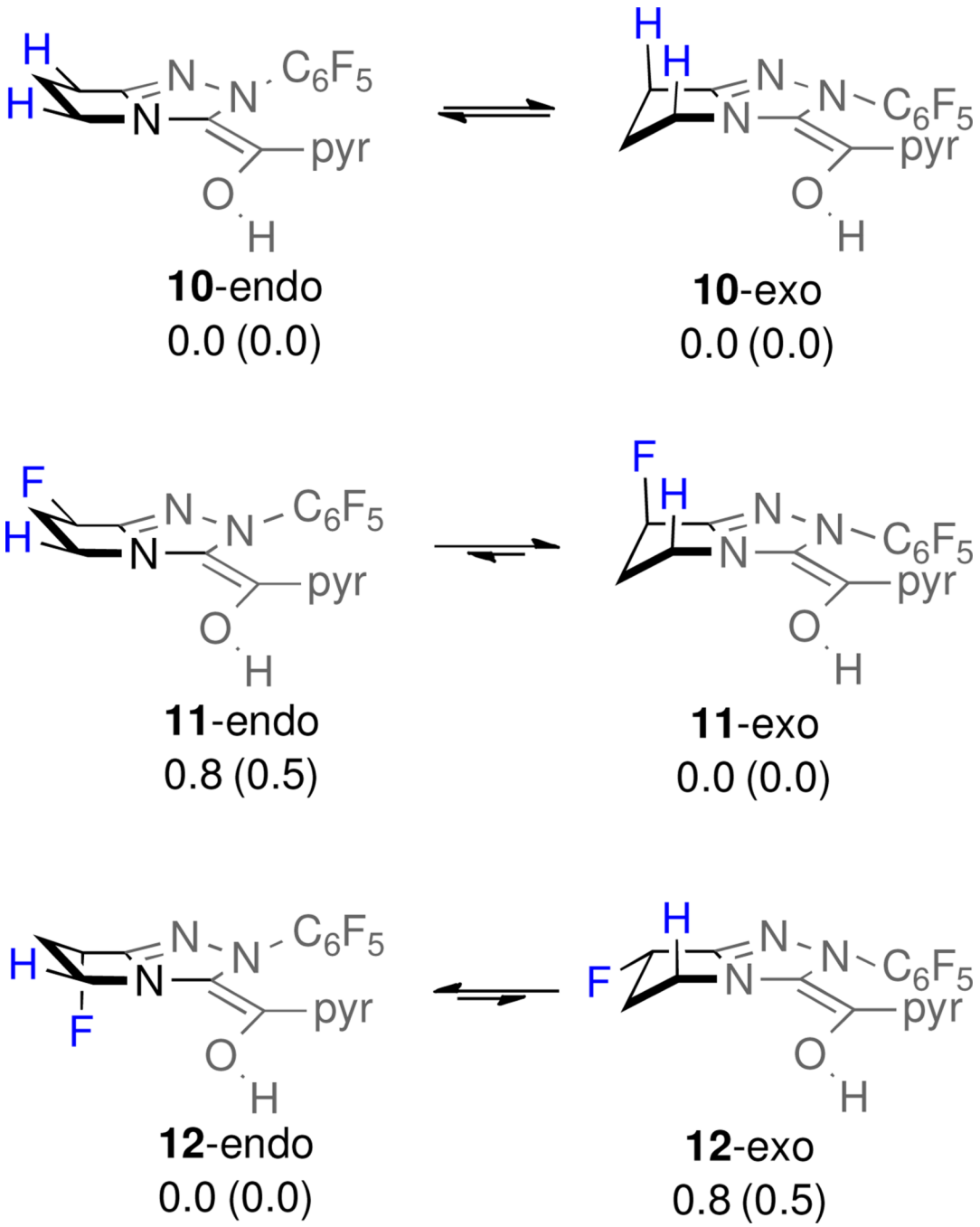

Figure 4.
B3LYP/6-31G(d) relative gas phase enthalpies of acyl anion equivalents **10–12**. B3LYP/6-31+G(d) relative enthalpies with solvation corrections (CPCM methanol) are in parentheses.

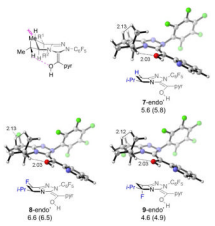

Figure 5.
Enol intermediates **7–9**-endo' and relative enthalpies with respect to **7–9**-exo. B3LYP/6-31+G(d) relative enthalpies with solvation corrections (CPCM methanol) are in parentheses.

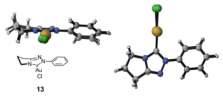

Figure 6.
Overlay of crystal structure and calculated structure (B3LYP/6-31G(d) for C, N, Cl and H, / LANL2DZ for gold) of **13**.

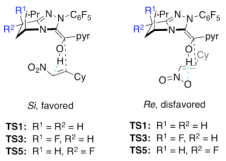

Figure 7.
Si-and *Re*-face transition structures.

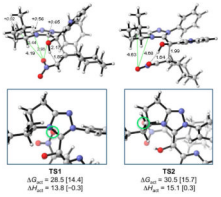

Figure 8.
B3LYP/6-31G(d) gas phase transition structures and $\Delta G^{\ddagger}$ for **7**. M06-2X/6-31+G(d) energies in brackets.

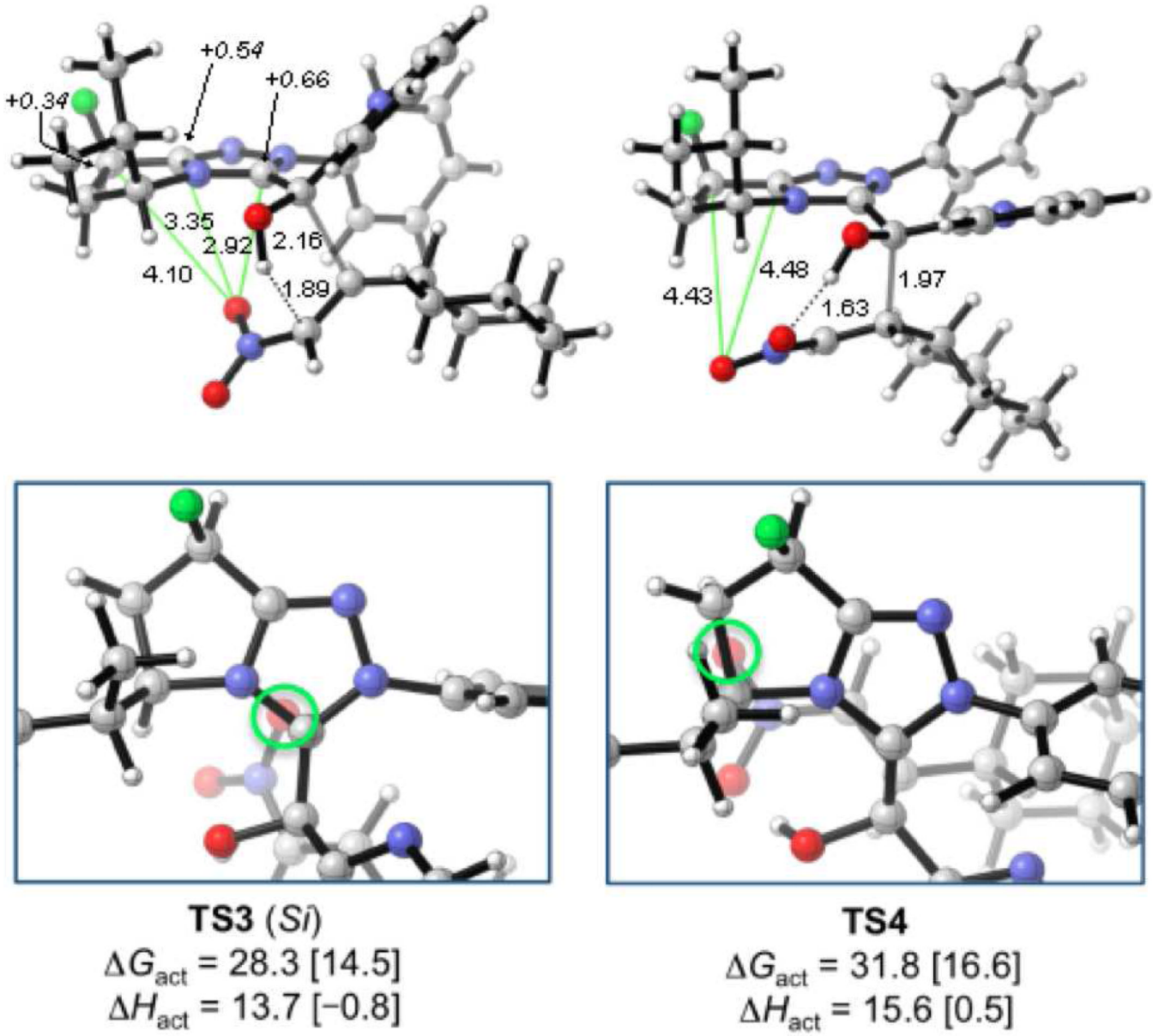

Figure 9.
B3LYP/6-31G(d) gas phase transition structures and $\Delta G^{\ddagger}$ for **8**. M06-2X/6-31+G(d) energies in brackets.

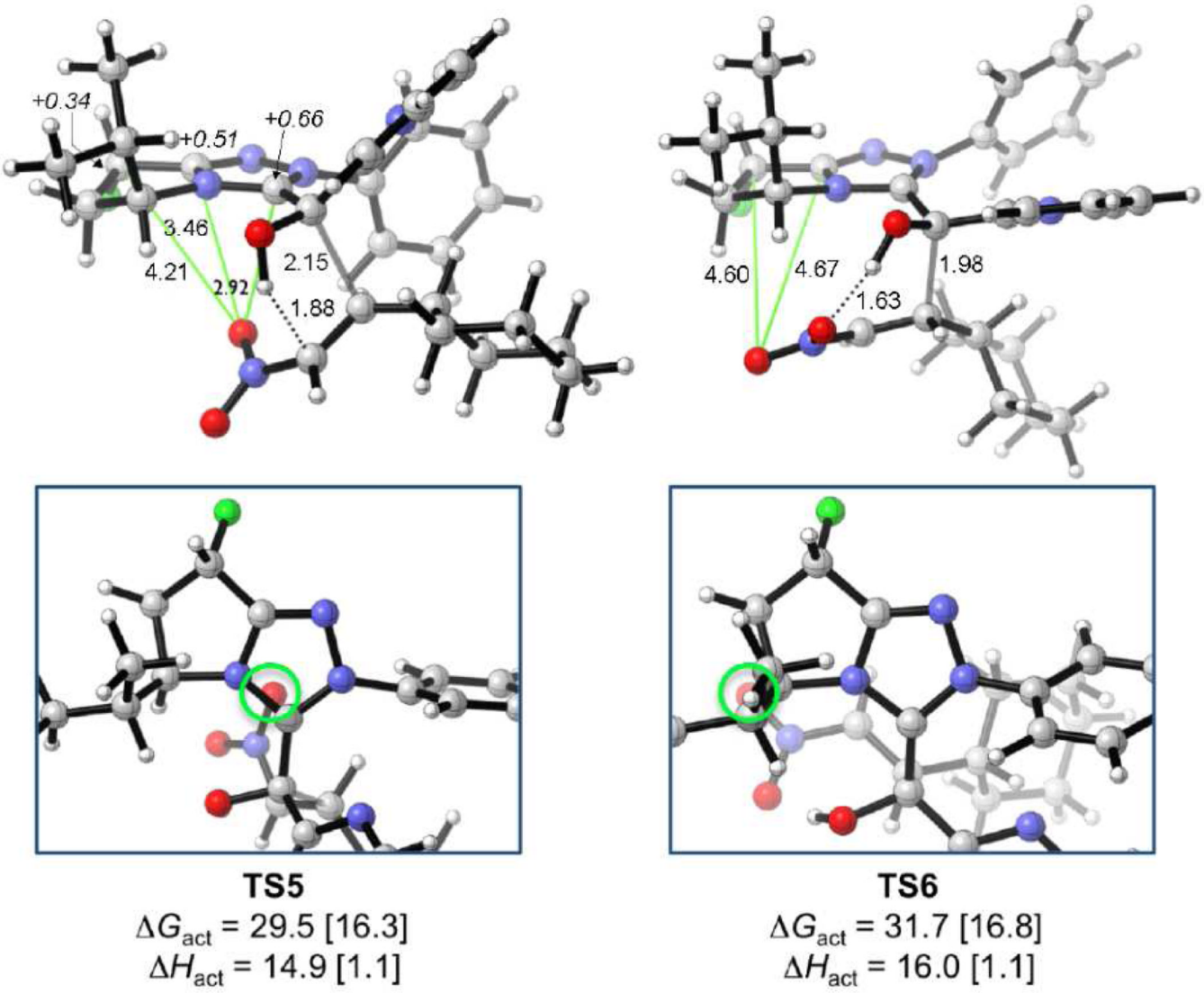

Figure 10.
B3LYP/6-31G(d) gas phase transition structures and $\Delta G^{\ddagger}$ for **9**. M06-2X/6-31+G(d) energies in brackets.

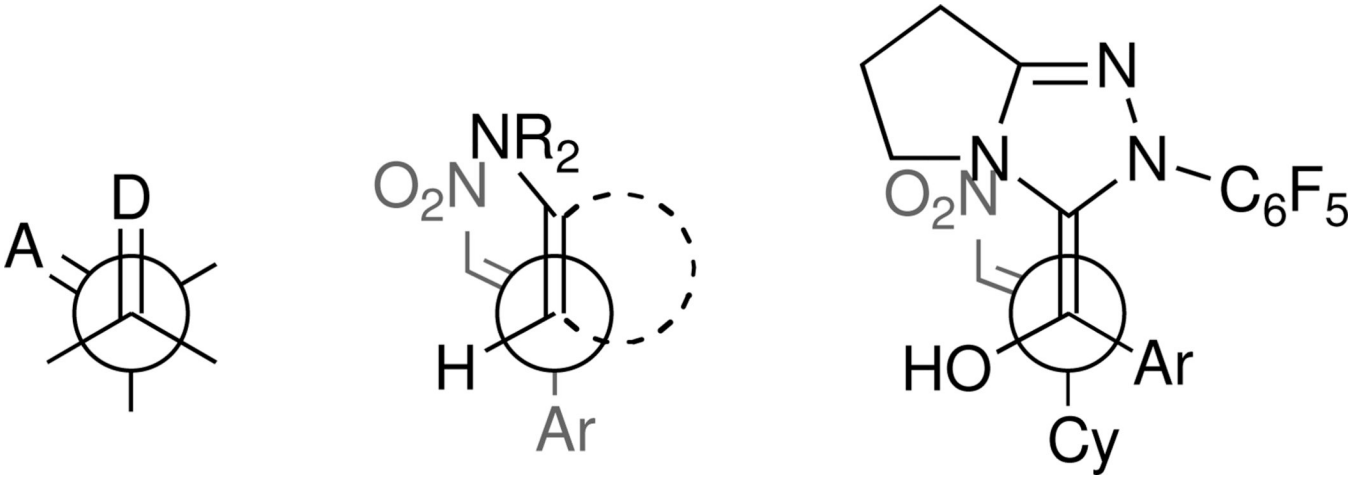

Figure 11.
Seebach's topological rule applied to the Stetter reaction

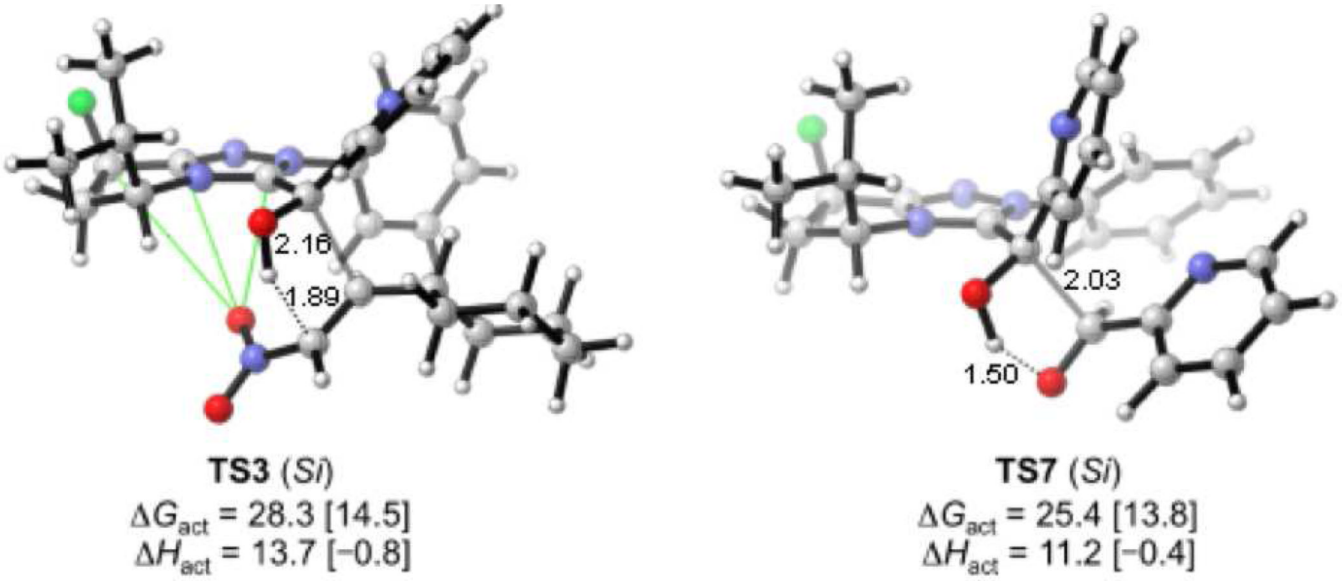

Figure 12.
Comparison of the transition states for the Stetter reaction, **TS3** (*Si*), and benzoin condensation, **TS7**. B3LYP/6-31G(d) gas phase transition structures and $\Delta G^{\ddagger}$. M06-2X/6-31+G(d) energies in brackets.

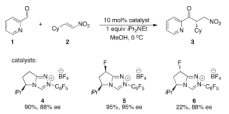

Scheme 1.

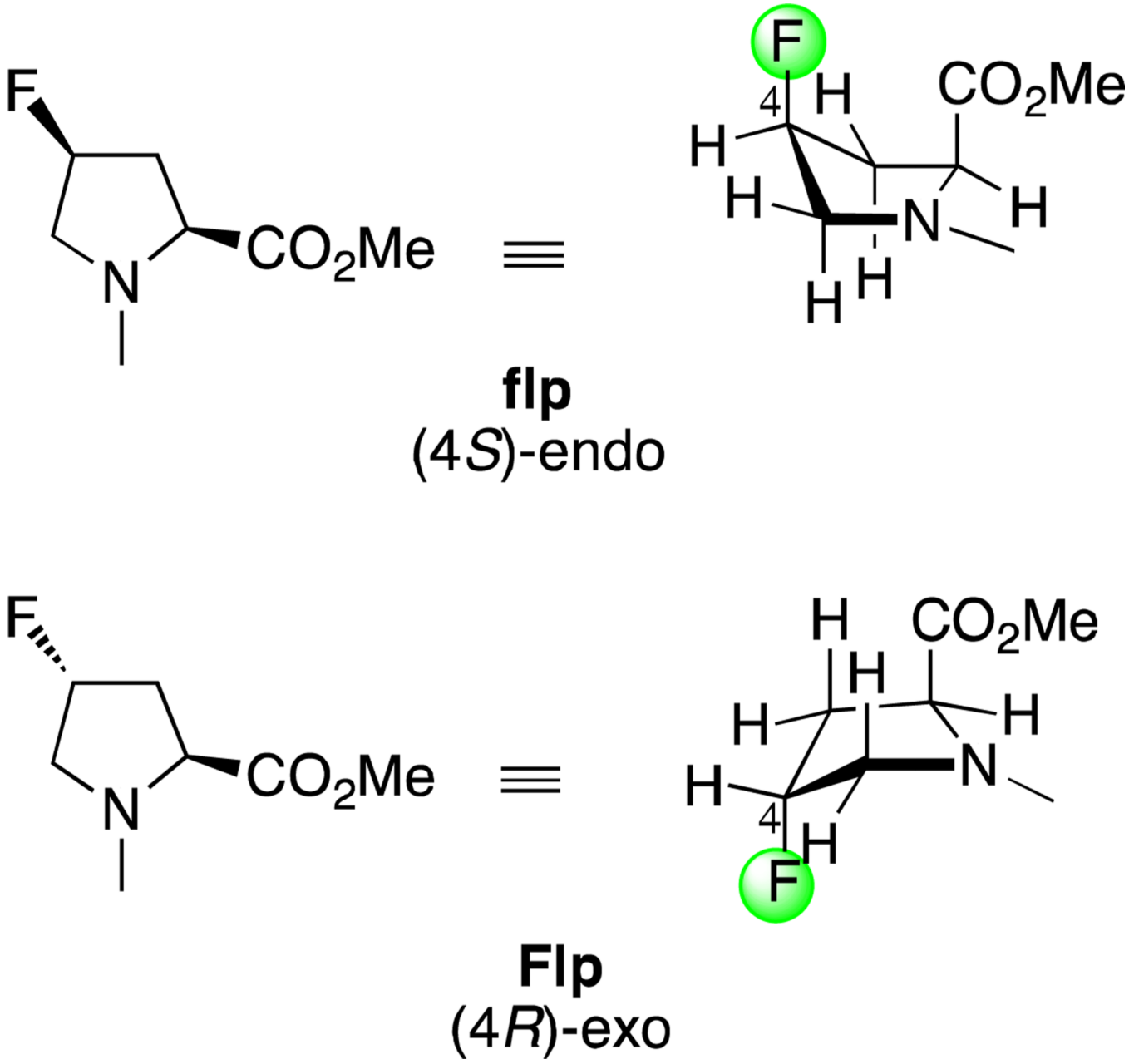

Scheme 2.
Proline conformations reported by Raines.

Table 1

Summary of calculated and experimental enantioselectivities[a]

entry	catalyst	experimental		B3LYP[b] gas phase		M06-2X [c] methanol		B3LYP [c] methanol	
		e.r.	$\Delta\Delta G^{\ddagger}$	e.r.	$\Delta\Delta G^{\ddagger}$	e.r.	$\Delta\Delta G^{\ddagger}$	e.r.	$\Delta\Delta G^{\ddagger}$
1	**4**	94:6	1.6	97:3	2.1	91:9	1.3	93:7	1.6
2	**5**	98:2	2.2	99:1	2.9	98:2	2.3	93:7	1.6
3	**6**	94:6	1.6	98:2	2.2	86:14	1.1	86:14	1.1

[a] Calculated enantioselectivities include 3–5 low-energy conformations. The free energy difference here is a weighted average of the energies of these conformations. The $\Delta\Delta G_{act}$ in Figures 8–10 involve only the lowest energy transition structure. See the Supporting Information.

[b] 6-31G(d) basis set.

[c] 6-31+G(d) basis set. Solvation single point energies on B3LYP/6-31G(d) geometries.

Table 2

F-N1 distances in **TS3–TS6**.

entry	TS	F-N1 (Å)
1	**TS3**	3.24
2	**TS4**	3.16
3	**TS5**	3.07
4	**TS6**	3.13